Quantification of myocardial perfusion SPECT using freeware package (cardioBull)

メタデータ	言語: eng
	出版者:
	公開日: 2017-10-03
	キーワード (Ja):
	キーワード (En):
	作成者:
	メールアドレス:
	所属:
URL	http://hdl.handle.net/2297/29527

[Original article]
Quantification of myocardial perfusion SPECT using freeware package (cardioBull)

Koichi Okuda[1], Kenichi Nakajima[2], Tetsuo Hosoya[3], Takehiro Ishikawa[3], Shinro Matsuo[2], Masaya Kawano[4], Junichi Taki[2], Seigo Kinuya[2]

1. Department of Biotracer Medicine, Kanazawa University Graduate School of Medical Science, Kanazawa, Japan
2. Department of Nuclear Medicine, Kanazawa University Hospital, Kanazawa, Japan
3. Fujifilm RI Pharma Co., Ltd., Tokyo, Japan
4. Department of Radiology, Weill Cornell Medical College of Cornell University, New York, NY

Koichi Okuda, Ph.D.
Department of Biotracer Medicine, Kanazawa University Graduate School of Medical Science
13-1 Takara-machi, Kanazawa, 920-8641, Japan
Tel +81-76 265 2333, Fax +81-76 234 4257,
E-mail: okuda@nmd.m.kanazawa-u.ac.jp

Secondary correspondence:
Kenichi Nakajima, MD.
Department of Nuclear Medicine, Kanazawa University Hospital
E-mail: nakajima@med.kanazawa-u.ac.jp

Abstract

Objective: We have developed freeware package for automatically quantifying myocardial perfusion and ^{123}I-labeled radiopharmaceutical single-photon emission computed tomography (SPECT), which is called "cardioBull". We aim to evaluate diagnostic performance of the detection of coronary artery disease (CAD) on the developed software in comparison with commercially available software package (Quantitative Perfusion SPECT (QPS)).

Methods: Stress-rest ^{99m}Tc-sestamibi myocardial perfusion SPECT was performed in 36 patients with CAD and 35 control patients. A ≥75% stenosis in the coronary artery was identified by coronary angiography in the CAD group. Segmental perfusion defect score was automatically calculated by both cardioBull and QPS software. Summed stress score (SSS) was obtained to detect CAD by the receiver operator characteristic (ROC) analysis. Areas under the ROC curves (AUC) were calculated in patient-based and coronary-based analyses.

Results: Mean SSSs showed no significant difference between cardioBull and QPS (6.0 ± 7.1 vs. 5.6 ± 7.0). The AUC for cardioBull was equivalent to that for QPS (0.91 ± 0.04 vs. 0.87 ± 0.04, *p* = n.s.). Sensitivity, specificity, and accuracy for cardioBull were 89%, 74%, and 82%, respectively. For the regional detection of CAD, the AUC showed largest value in LAD territory (0.86 ± 0.06 for cardioBull, 0.87 ± 0.06 for QPS, *p* = n.s.). Sensitivity, specificity and accuracy of cardioBull were 70%, 88%, and 83% for the LAD, 91%, 62%, and 66% for the LCx, and 78%, 69%, and 70% for the RCA, respectively.

Conclusions: The AUC, sensitivity, specificity and accuracy for the detection of CAD showed high diagnostic performance on the developed software. Additionally, the developed software provided comparable diagnostic performance to the commercially available software package.

Key Words: myocardial perfusion SPECT; automatic quantification; coronary artery disease; image processing

Introduction

Myocardial perfusion single-photon emission computed tomography (SPECT) is a non-invasive method for patients with suspected or known coronary artery disease (CAD) [1-2]. The visual interpretation of myocardial perfusion SPECT (MPS) has been performed to detect myocardial ischemia, therapeutic decision making, and prognostic estimates, although the visual interpretation is subjective and dependent on observer experience. To overcome these limitations, commercially available software packages such as 4D-MSPECT (University of Michigan Medical Center, Ann Arbor, MI, USA), Emory's Cardiac Toolbox (Emory University, Atlanta, GA, USA), and Quantitative Perfusion SPECT (QPS) (Cedars-Sinai Medical Center, Los Angeles, CA, USA) have provided quantitative and reproducible results in assessment of MPS study [3-7].

Though, differences of the sensitivity, specificity, and accuracy in the detection of CAD were observed among these software packages [8-9]. The difference of the scoring algorithm was also demonstrate in the assessment of the reversible perfusion defects using summed difference score (SRS) [10]. Moreover the considerable differences between QPS and 4D-MSPECT were observed in summed stress score (SSS) and SRS [11]. When we evaluate patients with serial MPS studies or results between different sites, the same software should be used in both cases.

In this study, to overcome the limitation, we have developed freeware for automatic quantification of MPS imaging, which is driven on a Windows platform. Our aim is to quantitatively evaluate the diagnostic performance of the detection of CAD with the developed software on angiographically validated patients.

Material and Methods

Study population

A total of 71 studies of 27 females and 44 males who underwent stress and rest gated ^{99m}Tc-sestamibi (MIBI) MPS with exercise (n=43) and adenosine (n=28) stress was selected in Kanazawa University. The study population included 27 with diabetes mellitus (38%), 37 with hypertension (52%) and 17 with hypercholesterolemia (23%). The subjects who had history of revascularization, myocardial infarction, non-ischemic cardiomyopathy, and valvular heart disease were excluded. Table 1 summarizes characteristics of CAD and control subjects. In the CAD group, all subjects underwent coronary angiography and a stenosis with 75% or greater narrowing was considered significant. Coronary angiography revealed single vessel disease (SVD) in 32 subjects, double vessel disease (DVD) in 4 subjects. The stenoses of left anterior descending coronary artery (LAD), left circumflex coronary artery (LCx), and right coronary artery (RCA) were observed 18, 7, and 7 in the SVD subjects, and 2, 4, and 2 in the DVD subjects, respectively. In the control group, coronary angiography was performed in 8 subjects, and the stenosis with less than 50% and 25%

were observed in 3 and 5 subjects, respectively. All the subjects were judged as normal stress/rest MPS by visual assessment in the control group.

Image acquisition

Both stress and rest MPS images were acquired at 40 minutes after injection of ^{99m}Tc MIBI of 300-370 MBq and 700-900 MBq, respectively. MPS acquisition was performed with a circular 360-degree acquisition with 60 projections at 35 seconds per projection by a three-head gamma camera (GCA-9300A/HG, Toshiba Medical Systems, Tokyo, Japan) equipped with a low-energy high-resolution collimator. A pixel size for a 64 x 64 matrix was 6.4 mm. A photopeak window of ^{99m}Tc was set as a 20% energy window centered at 140 keV, and neither scatter nor septal penetration windows were used. Division of RR interval was 16 frames in a gated acquisition. We anonymously exported the short-axis images using digital imaging and communications in medicine (DICOM) format to the developed software.

cardioBull

We developed fully automated software for the quantification of MPS, which was called "cardioBull". When the short-axis images are imported to the software, optimal apical and basal slices are automatically determined. For a qualitative polar map creation, an automatic co-registration is applied for a pair of the short-axis images [12]. A myocardial perfusion polar map is generated by using circumferential profile curve analysis with the apical radial sampling method [13]. Extent and severity maps are also generated automatically based on a normal database. A scoring algorithm for the evaluation of low uptake employs a 5-point scoring system as 0 - 4 for normal, mildly abnormal, moderately abnormal, severe abnormal, and perfusion defect, respectively. The polar map is segmented by 17 or 20 regions of the left ventricular (LV) model.

Three major algorithmic improvements of the developed software are count normalization, sub-segmental scoring method, and robust scoring threshold. First, when myocardial perfusion counts are translated into the % uptake, a normalization factor is determined by search for a maximum count in the polar map (Figure 1). In the developed method, the normalization factor is set as the averaged count in a normal myocardial area. This is because the highest count, for example due to the papillary muscle, affects the count distribution of the polar map and the normalization factor. In our preliminary analysis, all of the infracted or ischemic area showed lower counts < 70th percentile. Additionally, highest counts due to the papillary muscle were usually > 90th percentile of counts. Then, we determined 80 ± 10th percentile of myocardial perfusion count as a normal area. Second, we divide a segmental area of the polar map into sub-segmental areas and calculate sub-segmental perfusion defect scores. Subsequently the segmental perfusion defect score is determined by the average of the sub-segmental scores. This sub-segmental scoring method can provide the detail distribution of the perfusion defect scores in the segmental area, and avoid

underestimating the segmental score. Third, when the normal limit for perfusion abnormality is defined by the mean -2SD, and the defect perfusion is set as a mean × 50%, the scoring thresholds are determined to divide the range between the mean -2SD and mean × 50% into three severities. As for the conventional standard method, a threshold for the severity of hypoperfusion was determined based on the deviation of the normal database.

Data analysis

The short-axis images were reconstructed with filtered back projection method with a Butterworth filter (cutoff, 0.34 cycles/cm; order, 8) on GMS-5500A/PI workstation (Toshiba Medical Systems, Tokyo, Japan). SSS was derived from cardioBull and QPS (version 2008) on the 17-segment model of the polar map. Regional SSSs were also calculated in LAD (SSS_{LAD}), LCx (SSS_{LCx}), and RCA (SSS_{RCA}) territories. Combined quantitative index including the severity and extent was also defined and called as "% severity" in cardioBull. This index indicated summed % uptake below the normal limit divided by that below the average of the normal database with the pixel-by-pixel based analysis. The Japanese normal databases for MIBI MPS were utilized, which were created by the Japanese Society of Nuclear Medicine (JSNM) working group [14-18]. For the assessment of coronary angiogram, all coronary angiograms were visually and independently interpreted by at least two cardiology specialists in the Department of Cardiology.

Statistical analysis

All continuous values were expressed as mean ± standard deviation (SD) unless otherwise noted. A paired t test was used to analyze the differences in paired continuous data. Chi-square and McNemar tests were used to analyze the differences in discrete data. All statistical tests were two-tailed, and a p value of less than 0.05 was considered significant. Correlation and Bland-Altman analyses were used for the assessment of agreement. Receiver operator characteristic (ROC) analysis was utilized to evaluate the performance of the detection of the CAD depending on the area under the ROC curve (AUC), sensitivity, specificity and accuracy. AUC was expressed as area ± standard error. When we compared between AUCs, the method of DeLong et al. was used [19]. These analyses were performed by using MedCalc software version 11.2.1.0 (Mariakerte, Belgium).

Results

There was no significant difference of patient age between CAD and control subjects (68.0 ± 9.3 vs. 66.3 ± 10.1, p=n.s.). End-diastolic volume (EDV) and end-systolic volume (ESV) for the CAD group showed significantly higher values than that for the control group (110.7 ± 38.5 vs. 84.6

± 24.3 mL, 43.9 ± 25.2 vs. 30.2 ± 15.4 mL, p=0.0015, 0.0092, respectively).

Figure 2 shows the comparison of the scoring methods on a preliminary study. SSS derived from the standard scoring method; namely, using average count per segment, underestimated the severity of the CAD in comparison of the developed software and QPS. In the LAD territory, SSS_{LAD} for the developed method, standard method and QPS were 6, 4, and 8, respectively. The developed method could detect the 75 % stenosis of the atrioventricular nodal branch at the apical inferior region as score 1 on the polar map b.

Mean SSSs were 6.0 ± 7.1 for cardioBull and 5.6 ± 7.0 for QPS (p = n.s.). A linear regression line of SSS between cardioBull and QPS was calculated as y = 1.06 + 0.87 x, r = 0.86, p < 0.0001 (Figure 3a). When the agreement between cardioBull and QPS was assessed by Bland-Altman analysis, the mean difference of SSS was 0.3, and the 95% limits of agreement ranged from -6.9 to 7.6. Figure 4a shows the ROC curves of the detection of CAD by cardioBull and QPS. The AUC for cardioBull was equivalent to that for QPS (0.91 ± 0.04 vs. 0.87 ± 0.04, p = n.s.). When applying the threshold of SSS ≥ 3, sensitivity, specificity and accuracy are shown in Figure 5. Sensitivity for cardioBull was higher than that for QPS (89% vs. 75%), although no significantly difference was found between cardioBull and QPS.

The mean scores of SSS_{LAD}, SSS_{LCx}, and SSS_{RCA} were 2.1 ± 4.0, 2.3 ± 3.0, and 1.6 ± 2.2 for cardioBull, and 2.0 ± 4.1, 2.1 ± 3.1, and 1.3 ± 2.1 for QPS, respectively (p = n.s. for all). The correlation was highest for LAD territory, and lowest for RCA territory (r = 0.95, 0.66, respectively) (Figure 3). The mean differences showed almost zero, and the 95% limits of agreements ranged from -2.6 to 2.6 for SSS_{LAD}, -3.6 to 3.9 for SSS_{LCx}, and -3.3 to 3.7 for SSS_{RCA} in the Bland-Altman analyses, respectively. The AUC was highest for LAD territory and lowest for RCA territory (0.86 ± 0.06 and 0.77 ± 0.08 for cardioBull, and 0.87 ± 0.06 and 0.76 ± 0.10 for QPS, respectively) (Figure 4). When applying the thresholds of SSS_{LAD}, SSS_{LCx}, and SSS_{RCA} ≥ 2, sensitivity, specificity, and accuracy of cardioBull were 70%, 88%, and 83% for the LAD, 91%, 62%, and 66% for the LCx, and 78%, 69%, and 70% for the LCx, respectively (Figure 6). Sensitivity, specificity, and accuracy for QPS showed higher values than that for cardioBull in LAD territory, although there were no significant differences between QPS and cardioBull.

Mean stress % severity showed 2.0 ± 4.0. Relationship between % severity (y) and SSS (x) showed good correlation (y = -0.16 + 0.14x + 0.01 × (x - 3.58)^2, r = 0.97, p < 0.0001). When the % total myocardial ischemia was set as 10% on the 17-segment model (SSS = 7), % severity corresponded to 1.0 %. The AUC did not significantly differ between % severity and SSS (0.909 ± 0.033 vs. 0.905 ± 0.035, respectively).

Discussion

In this study, we developed software for quantifying MPI, which automatically determined the LV myocardium and calculated SSS, SDS, and SRS based on a normal database. The aim of this

study is to evaluate the diagnostic performance of the detection of CAD in patient-based and coronary-based analyses. According to the results of correlation, Bland-Altman analyses, ROC curves, and AUCs, the developed software could provide the quantitative results with high diagnostic performance of the detection of CAD.

Quantitative software packages have provided high diagnostic performances of the detection of CAD. Slomka et al. evaluated the diagnostic performance of QPS in angiographically validated 256 patients [20]. When the subjects with the stenosis with 70% or greater narrowing were enrolled, the AUC for the detection of CAD was 0.89. Sensitivity, specificity and accuracy were 92%, 79%, and 88%, respectively. Nakajima et al. also evaluated the diagnostic performance of QPS with Japanese normal databases in angiographically validated consecutive 90 patients [18]. The AUC was 0.84 (≥ 75% stenosis), and sensitivity, specificity and accuracy were 79%, 72%, and 76%, respectively. In comparison with the previous studies, the developed software could provide high AUC of 0.91. As for the assessment of coronary-based analysis, Wolak et al. reported the AUCs for LAD, LCx, and RCA territories were 0.87, 0.79 and 0.76, respectively [8]. Guner et al. also showed those of LAD, LCx, and RCA were 0.71, 0.79, and 0.74, respectively [9]. The AUCs from the developed software showed similar to those from the previous studies in the coronary-based analysis.

The optimal count normalization is one of the most important factors in the quantitative assessment of MPS using normal databases. In the standard count normalization, the maximum count is adopted to normalize the whole counts in the polar map. The anterolateral count of the polar map frequently shows a higher value in the normal MPS. Thereby, a deviation may be underestimated at the anterolateral region when creating the normal database using maximum normalization technique (Figure 7). As for the developed method, the optimal normalization factor is determined by searching for the normal myocardium after excluding the hot regions. This technique can provide the accurate estimation of the deviation on the normal database. Therefore, normal limits (mean -2SD) of the developed technique are lower than that from the conventional normalization technique. Then, incidence of false positive detection of the lateral wall could be decreased.

Quantitative evaluation of Iodine-123 (^{123}I)-labeled meta-iodobenzylguanidine (MIBG) and beta-methyl-p-iodophenyl-pentadecanoic acid (BMIPP) SPECT can be performed with the developed software. Furthermore, quantitative evaluation of both MPS and ^{123}I radiopharmaceutical SPECT imaging also can be simultaneously performed by using the software. In the assessment of myocardial washout of MIBI, the developed software can provide regional washout values on the polar map. Tanaka et al. reported a quantitative regional washout index had high diagnostic performances than visual assessment in patients with angina or acute myocardial infarction [21]. Normal databases for [123]I- MIBG and BMIPP SPECT have recently been established [14, 16]. Then, these databases became available on the developed software and commercially available software packages. Moreover, using the database generation tool which included in the developed software package, we can construct databases for attenuation correction and prone imaging [22], and utilize

them for quantitative assessment of attenuation corrected and prone MPS imaging.

As a limitation in our study, since no patients with triple vessel disease (TVD) were included in the CAD group, the diagnostic performance with SVD, DVD, and TVD patients would be changed. Additionally, if the attenuation, scatter, and resolution corrections were applied to the MPS images, diagnostic performance for the detection of CAD would improve [23-26]. When we assessed the diagnostic performance of coronary artery territory, regional myocardial areas were utilized and categorized into three areas such as LAD (segments 1,2,7,8,13,14 and 17), LCx (segments 5,6,11,12 and 16) and RCA (segments 3,4,9,10 and 15). This LV segmentation, however, sometimes did not fit for the culprit lesion. The reader should take this disagreement into consideration in clinical use. QPS has an automatic modification function of incorrect LV segmentation.

Conclusion

We developed freeware for automatic quantification of MPS imaging with the normal database. The sensitivity, specificity, and accuracy showed high diagnostic performance on the detection of CAD. The developed software provided comparable diagnostic performance to the commercially available software package.
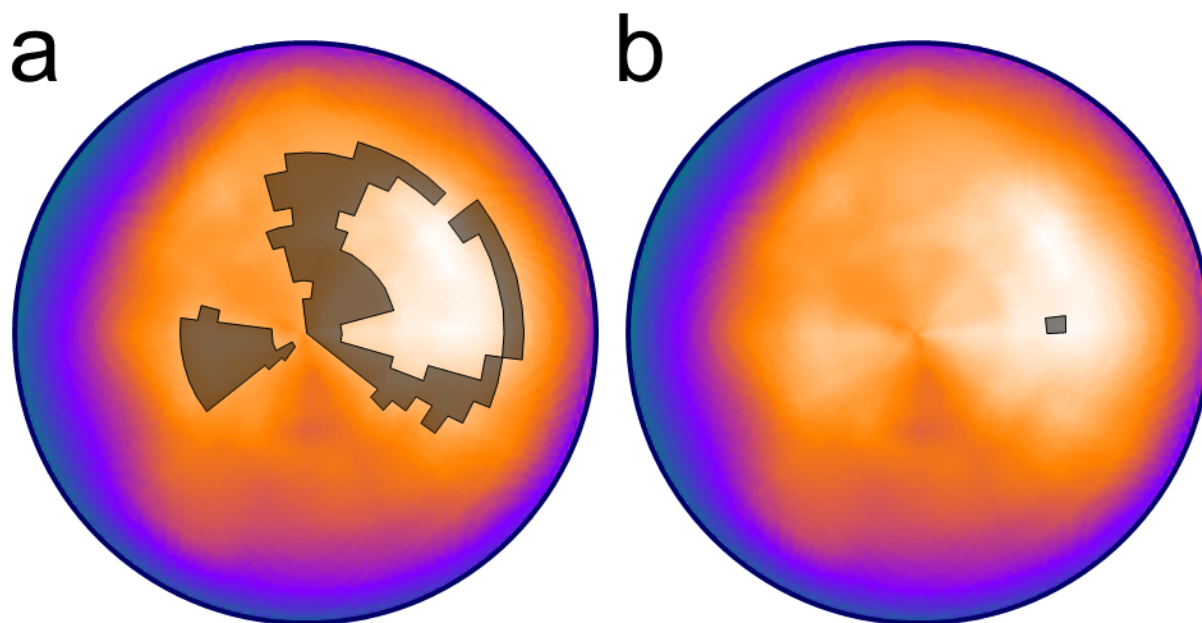
Acknowledgement

Figure 1. Comparison of reference areas for normalization in the developed and standard methods. **a**, Developed method: reference area is determined by normal myocardial perfusion counts between 70th and 90th percentiles (*painted dark gray*). **b**, Standard method: reference point is defined as a maximum perfusion count.
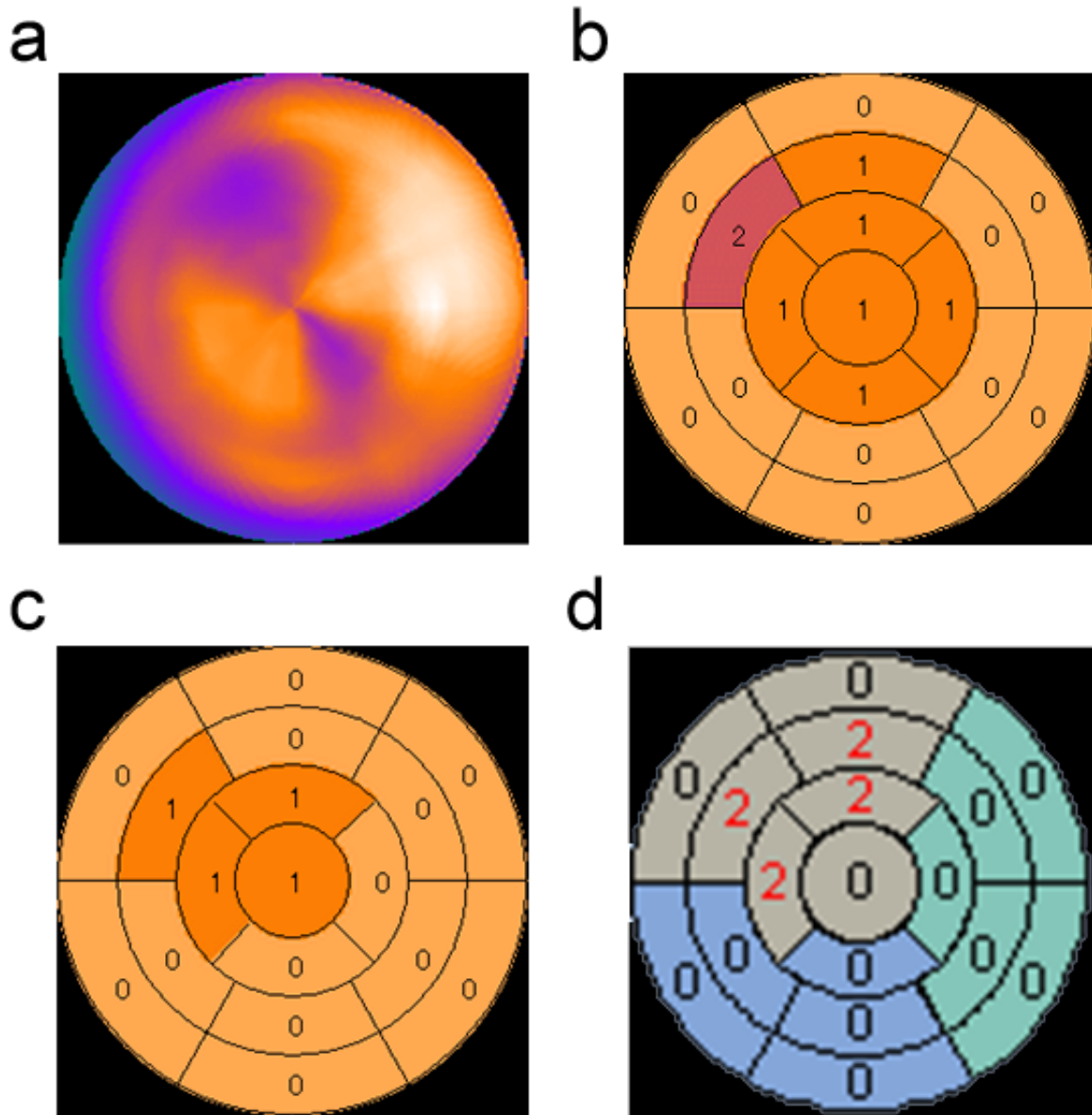
Figure 2. Comparison of the scoring results for the developed method, the standard method, and QPS. Study of an 82-year-old male with 75% and 90% stenoses at the atrioventricular nodal branch of the right coronary artery and the left anterior descending artery, respectively. **a,** Perfusion map. **b,** Developed method (SSS = 8). **c,** Standard method (SSS=4). **d,** QPS (SSS = 8)
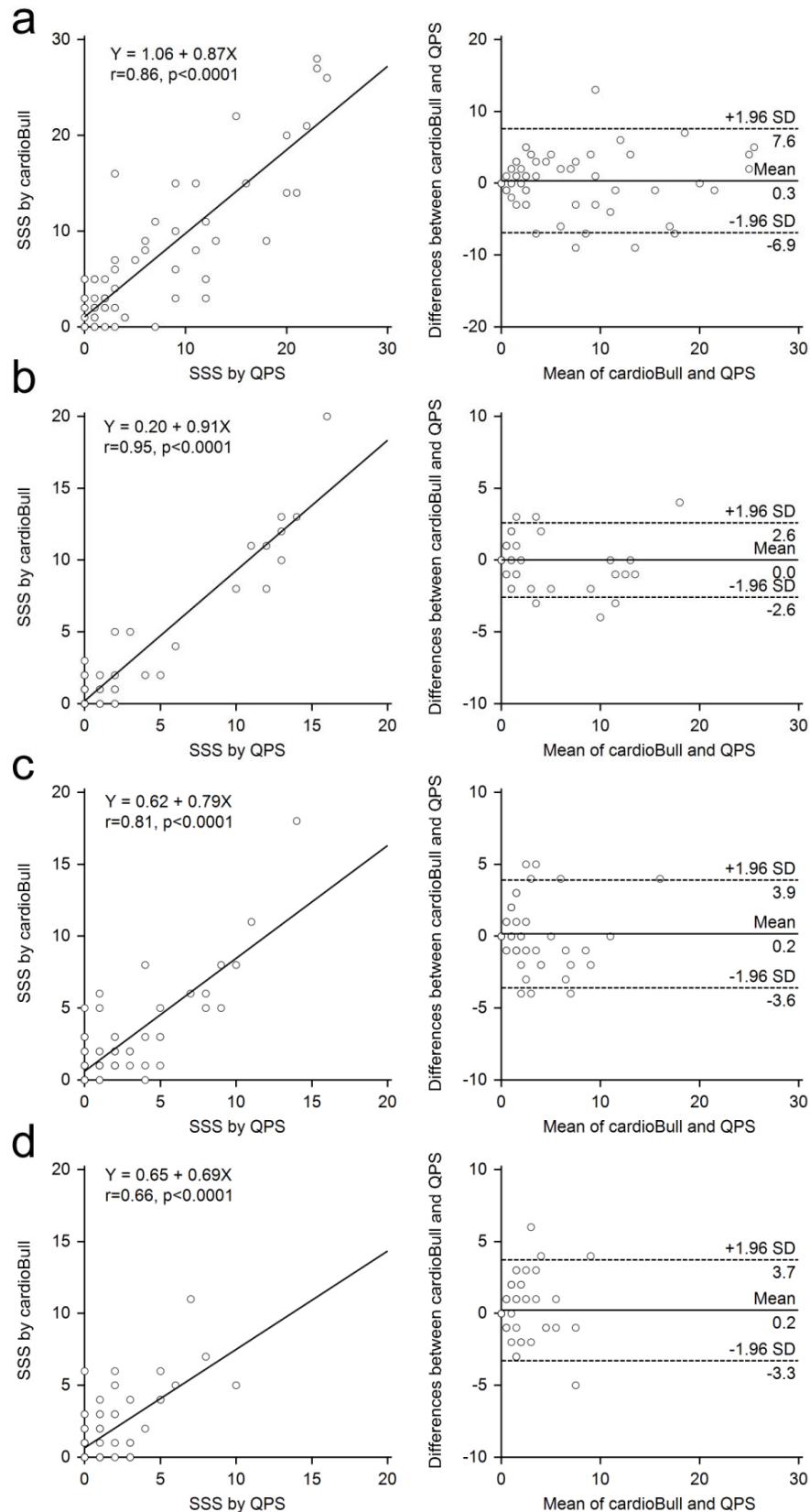
Figure 3. Relationship and agreement of SSS between cardioBull and QPS. **a,** Patient-based analysis. **b,** Coronary based analysis in LAD territory. **c,** Coronary based analysis in LCx territory. **d,** Coronary based analysis in RCA territory.
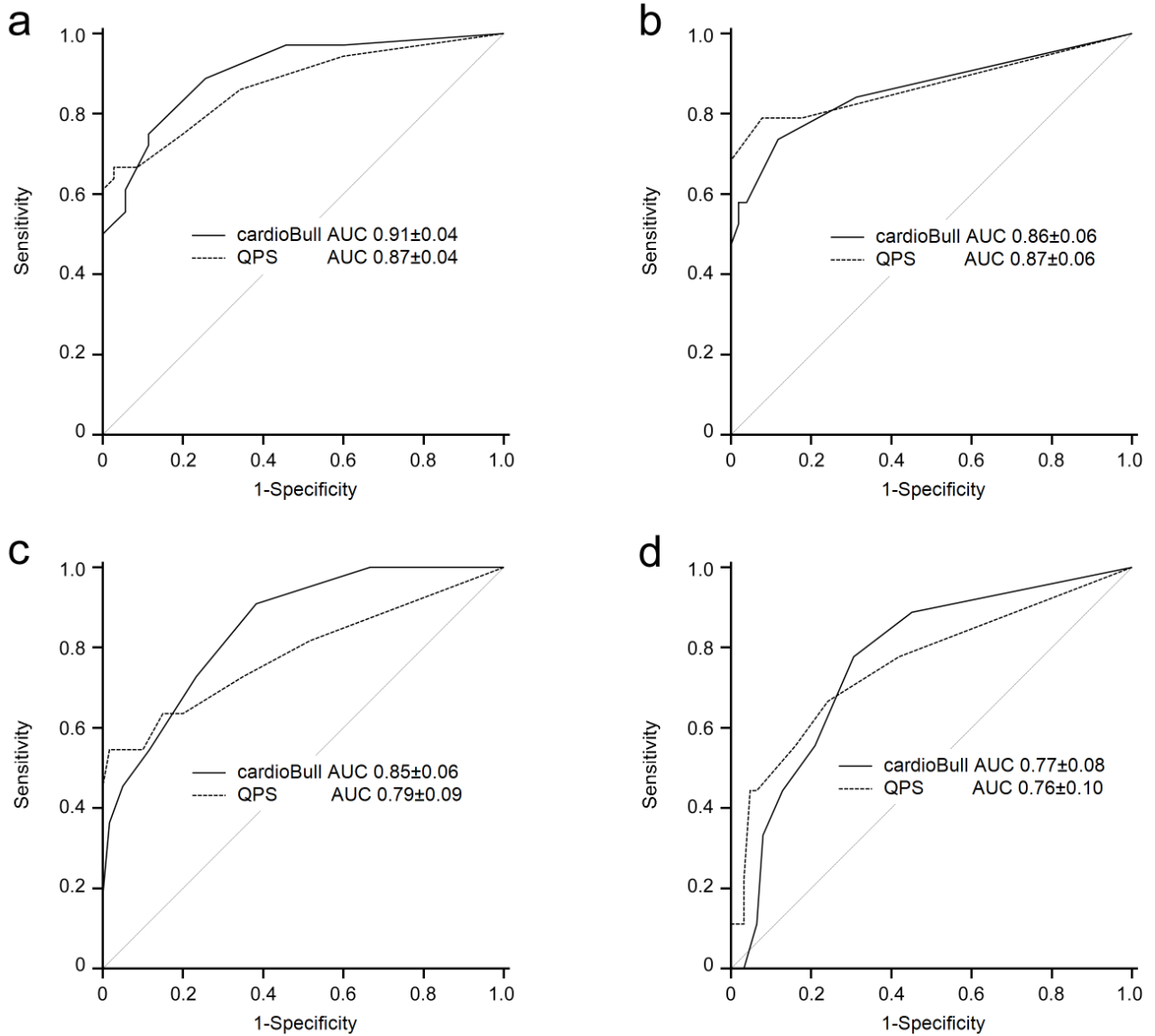
Figure 4. Comparison of ROC curves for the detection of CAD by cardioBull and QPS. **a**, Patient-based analysis. **b**, LAD territory. **c**, LCx territory. **d**, RCA territory.
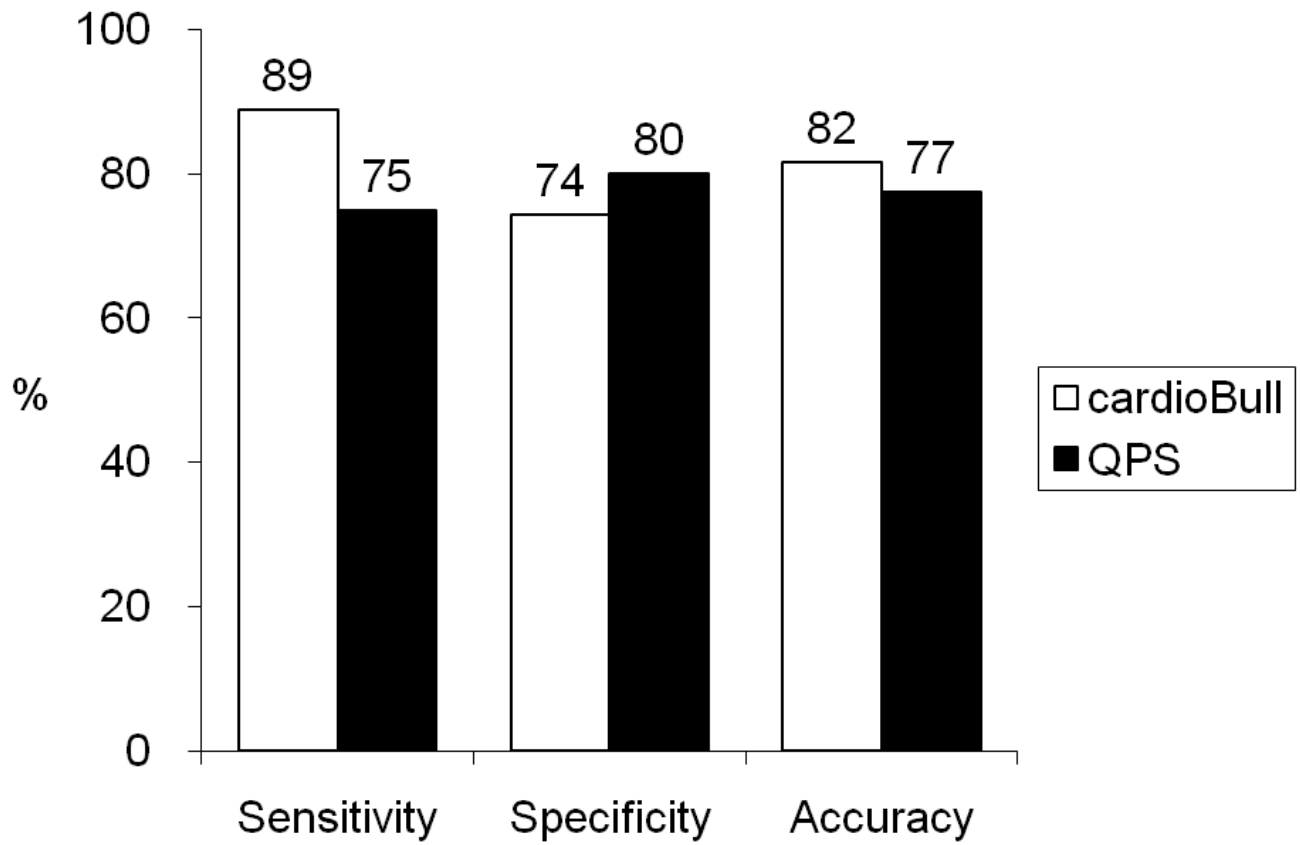
Figure 5. Sensitivity, specificity and accuracy for the detection of CAD by cardioBull and QPS in patient-based analysis.
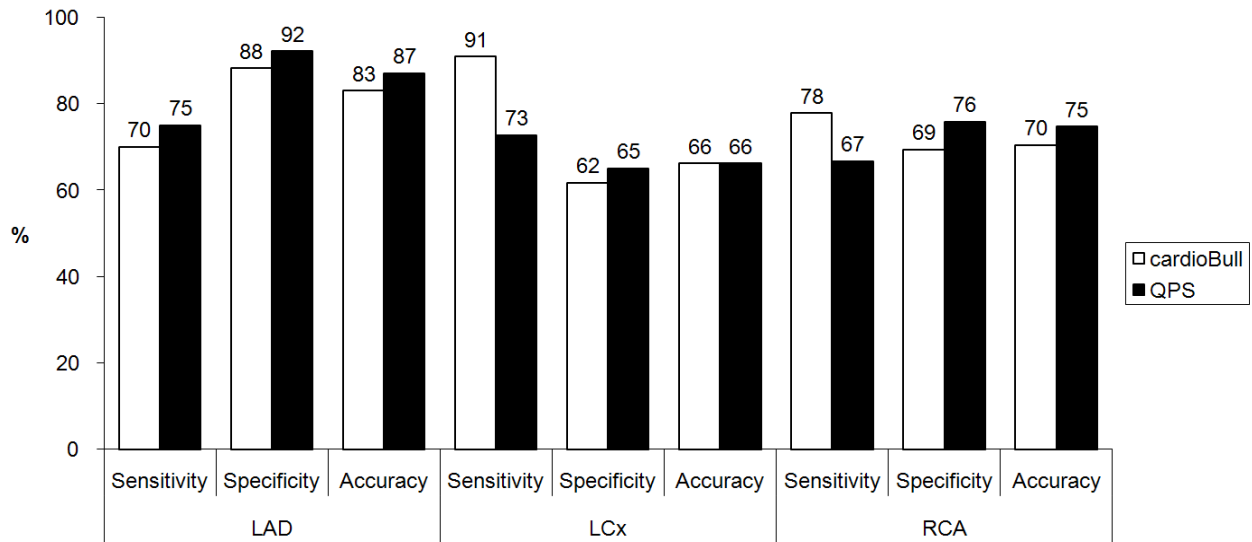
Figure 6. Sensitivity, specificity and accuracy for the detection of CAD by cardioBull and QPS in LAD, LCx and RCA territories.
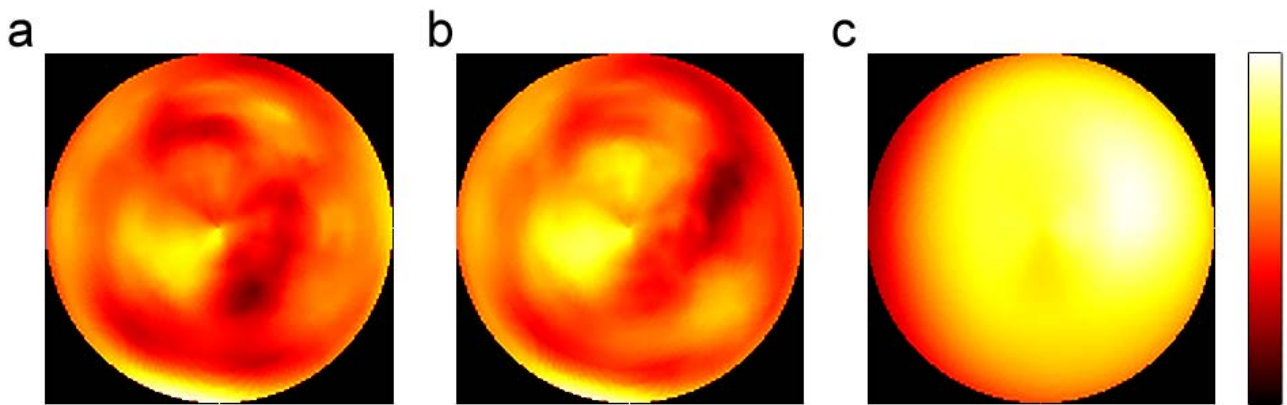
Figure 7. Comparison of deviation maps of normal databases derived from 10 healthy male subjects using the developed (**a**) and standard (**b**) methods. The lower value of the SD from the standard method is observed at the anterolateral region corresponded to the area of maximum count in mean maps (**c**) of normal database.

Table 1. Characteristics of subjects

Parameter	CAD group	Control group
Total	36	35
Female / Male	9 / 27	18 / 17
Age	68.0 ± 9.3	66.2 ± 10.3
gated SPECT data		
LVEF (%)	62.2 ± 10.6	66.3 ± 10.1
EDV (mL)	110.7 ± 38.5	84.6 ± 24.3
ESV (mL)	43.9 ± 25.2	30.2 ± 15.4
Angiographic data (≥ 75% stenosis)		
Single vessel	32 (89 %)	0
LAD territory	18	-
LCx territory	7	-
RCA territory	7	-
Double vessel	4 (11 %)	0
LAD territory	2	-
LCx territory	4	-
RCA territory	2	-
Triple vessel	0 (0 %)	0

LVEF left ventricular ejection fraction, *EDV* end-diastolic volume, *ESV* end-systolic volume, *LAD* left anterior descending coronary artery, *LCx* left circumflex coronary artery, *RCA* right coronary artery

References

1.	Klocke FJ, Baird MG, Lorell BH, Bateman TM, Messer JV, Berman DS, et al. ACC/AHA/ASNC guidelines for the clinical use of cardiac radionuclide imaging--executive summary: a report of the American College of Cardiology/American Heart Association Task Force on Practice Guidelines (ACC/AHA/ASNC Committee to Revise the 1995 Guidelines for the Clinical Use of Cardiac Radionuclide Imaging). Circulation. 2003;108:1404-18.

2.	Tamaki N. Guidelines for clinical use of cardiac nuclear medicine (JCS 2005). Circ J. 2005;69(Suppl. IV):1125-202.

3.	Ficaro EP, Lee BC, Kritzman JN, Corbett JR. Corridor4DM: the Michigan method for quantitative nuclear cardiology. J Nucl Cardiol. 2007;14:455-65.

4.	Garcia EV, Faber TL, Cooke CD, Folks RD, Chen J, Santana C. The increasing role of quantification in clinical nuclear cardiology: the Emory approach. J Nucl Cardiol. 2007;14:420-32.

5.	Germano G, Kavanagh PB, Slomka PJ, Van Kriekinge SD, Pollard G, Berman DS. Quantitation in gated perfusion SPECT imaging: the Cedars-Sinai approach. J Nucl Cardiol. 2007;14:433-54.

6.	Dostbil Z, Ariturk Z, Cil H, Elbey MA, Tekbas E, Yazici M, et al. Comparison of left ventricular functional parameters obtained from three different commercial automated software cardiac quantification program packages and their intraobserver reproducibility. Ann Nucl Med. 2011;25:125-31.

7.	Berman DS, Kang X, Gransar H, Gerlach J, Friedman JD, Hayes SW, et al. Quantitative assessment of myocardial perfusion abnormality on SPECT myocardial perfusion imaging is more reproducible than expert visual analysis. J Nucl Cardiol. 2009;16:45-53.

8.	Wolak A, Slomka PJ, Fish MB, Lorenzo S, Acampa W, Berman DS, et al. Quantitative myocardial-perfusion SPECT: comparison of three state-of-the-art software packages. J Nucl Cardiol. 2008;15:27-34.

9.	Guner LA, Karabacak NI, Cakir T, Akdemir OU, Kocaman SA, Cengel A, et al. Comparison of diagnostic performances of three different software packages in detecting coronary artery disease. Eur J Nucl Med Mol Imaging. 2010;37:2070-8.

10.	Svensson A, Akesson L, Edenbrandt L. Quantification of myocardial perfusion defects using three different software packages. Eur J Nucl Med Mol Imaging. 2004;31:229-32.

11.	Knollmann D, Knebel I, Koch KC, Gebhard M, Krohn T, Buell U, et al. Comparison of SSS and SRS calculated from normal databases provided by QPS and 4D-MSPECT manufacturers and from identical institutional normals. Eur J Nucl Med Mol I. 2008;35:311-8.

12.	Maes F, Collignon A, Vandermeulen D, Marchal G, Suetens P. Multimodality image registration by maximization of mutual information. IEEE Trans Med Imaging. 1997;16:187-98.

13.	Lin GS, Hines HH, Grant G, Taylor K, Ryals C. Automated quantification of myocardial ischemia and wall motion defects by use of cardiac SPECT polar mapping and 4-dimensional surface rendering. J Nucl Med Technol. 2006;34:3-17.

14.   Nakajima K. Normal values for nuclear cardiology: Japanese databases for myocardial perfusion, fatty acid and sympathetic imaging and left ventricular function. Ann Nucl Med. 2010;24:125-35.

15.   Akhter N, Nakajima K, Okuda K, Matsuo S, Yoneyama T, Taki J, et al. Regional wall thickening in gated myocardial perfusion SPECT in a Japanese population: effect of sex, radiotracer, rotation angles and frame rates. Eur J Nucl Med Mol Imaging. 2008;35:1608-15.

16.   Matsuo S, Nakajima K, Yamashina S, Sakata K, Momose M, Hashimoto J, et al. Characterization of Japanese standards for myocardial sympathetic and metabolic imaging in comparison with perfusion imaging. Ann Nucl Med. 2009;23:517-22.

17.   Nakajima K, Matsuo S, Kawano M, Matsumoto N, Hashimoto J, Yoshinaga K, et al. The validity of multi-center common normal database for identifying myocardial ischemia: Japanese Society of Nuclear Medicine working group database. Ann Nucl Med. 2009;24:99-105.

18.   Nakajima K, Okuda K, Kawano M, Matsuo S, Slomka P, Germano G, et al. The importance of population-specific normal database for quantification of myocardial ischemia: comparison between Japanese 360 and 180-degree databases and a US database. J Nucl Cardiol. 2009;16:422-30.

19.   DeLong ER, DeLong DM, Clarke-Pearson DL. Comparing the areas under two or more correlated receiver operating characteristic curves: a nonparametric approach. Biometrics. 1988;44:837-45.

20.   Slomka PJ, Nishina H, Berman DS, Akincioglu C, Abidov A, Friedman JD, et al. Automated quantification of myocardial perfusion SPECT using simplified normal limits. J Nucl Cardiol. 2005;12:66-77.

21.   Tanaka R, Simada K. Approach to establishment of a standard index for regional washout of a myocardial perfusion agent. Ann Nucl Med. 2010;24:713-9.

22.   Nishina H, Slomka PJ, Abidov A, Yoda S, Akincioglu C, Kang X, et al. Combined supine and prone quantitative myocardial perfusion SPECT: method development and clinical validation in patients with no known coronary artery disease. J Nucl Med. 2006;47:51-8.

23.   Ficaro EP, Fessler JA, Shreve PD, Kritzman JN, Rose PA, Corbett JR. Simultaneous transmission/emission myocardial perfusion tomography. Diagnostic accuracy of attenuation-corrected 99mTc-sestamibi single-photon emission computed tomography. Circulation. 1996;93:463-73.

24.   Utsunomiya D, Tomiguchi S, Shiraishi S, Yamada K, Honda T, Kawanaka K, et al. Initial experience with X-ray CT based attenuation correction in myocardial perfusion SPECT imaging using a combined SPECT/CT system. Ann Nucl Med. 2005;19:485-9.

25.   Okuda K, Nakajima K, Motomura N, Kubota M, Yamaki N, Maeda H, et al. Attenuation correction of myocardial SPECT by scatter-photopeak window method in normal subjects. Ann Nucl Med. 2009;23:501-6.

26.   Tashiro K, Tomiguchi S, Shiraishi S, Yoshida M, Sakaguchi F, Yamashita Y. Clinical usefulness of a collimator distance dependent resolution recovery in myocardial perfusion SPECT:

a clinical report from a single institute. Ann Nucl Med. 2011;25:133-7.